Hindawi
International Journal of Photoenergy
Volume 2020, Article ID 8877744, 7 pages
https://doi.org/10.1155/2020/8877744

Research Article

Thickness Dependence of Window Layer on $CH_3NH_3PbI_{3-X}Cl_X$ Perovskite Solar Cell

Wycliffe Isoe,[1] **Maxwell Mageto**,[1,2] **Christopher Maghanga**,[2,3] **Maurice Mwamburi**,[4] **Victor Odari**,[1,2] **and Celline Awino**[1,2]

[1]*Department of Physics, Masinde Muliro University of Science and Technology, P.O. Box 190-50100 Kakamega, Kenya*
[2]*Materials Research Society of Kenya, P.O. Box 15653-00503 Nairobi, Kenya*
[3]*Department of Physical & Biological Sciences, Kabarak University, P.O. Box Private Bag Kabarak, Nakuru, Kenya*
[4]*Department of Physics, University of Eldoret, P.O. Box 1125 Eldoret, Kenya*

Correspondence should be addressed to Wycliffe Isoe; isoewycliffe@gmail.com

Received 26 May 2020; Accepted 11 July 2020; Published 28 July 2020

Academic Editor: Alberto Álvarez-Gallegos

$CH_3NH_3PbI_{3-x}Cl_x$ has been studied experimentally and has shown promising results for photovoltaic application. To enhance its performance, this study investigated the effect of varying thickness of FTO, TiO_2, and $CH_3NH_3PbI_{3-x}Cl_x$ for a perovskite solar cell with the structure glass/FTO/TiO_2/$CH_3NH_3PbI_{3-x}Cl_x$/Spiro-OMeTAD/Ag studied using SCAPS-1D simulator software. The output parameters obtained from the literature for the device were 26.11 mA/cm^2, 1.25 V, 69.89%, and 22.72% for J_{sc}, V_{oc}, FF, and η, respectively. The optimized solar cell had a thickness of 100 nm, 50 nm, and 300 nm for FTO, TiO_2, and $CH_3NH_3PbI_{3-x}Cl_x$ layers, respectively, and the device output were 25.79 mA/cm^2, 1.45 V, 78.87%, and 29.56% for J_{sc}, V_{oc}, FF, and η, respectively, showing a remarkable increase in FF by 8.98% and 6.84% for solar cell efficiency. These results show the potential of fabricating an improved $CH_3NH_3PbI_{3-x}Cl_x$ perovskite solar cell.

1. Introduction

The demand for energy is on an increasing trend. This is characterized by the speedy technological advancement and rapid growth of the economy globally. The world population is also growing rapidly and thus primary sources of energy will be exhausted if an effective alternative source of energy is not sought. The oil reservoirs, coal, as well that of the gas will completely be exploited in the next 35 years, 107 years, and 37 years, respectively [1]. Furthermore, the burning of fossil fuels has significantly contributed to environmental pollution and global warming [2]. Therefore, there is a need to find a clean, renewable, and sustainable alternative source of energy. Solar energy has for a long time been considered among the best alternative source of energy owing to its abundance but harvesting and conversion technology has been the limiting factor. For decades, silicon has remained the dominant material for the production of commercial solar conversion devices. Research seems to suggest that perovskites stand to be good candidates among other materials [3, 4].

Perovskite solar cells (PSCs) have attracted much attention in the field of photovoltaic due to their high light absorption, tunable band-gap energy, high open-circuit voltage, easy synthesis and fabrication, low cost, good thermal stability, and high efficiency [5–8]. In the past 10 years, the efficiency of PSCs has greatly improved from about 2.2% to more than 22% [9]. The understanding of the operational mechanism of the PSCs is necessary for further improvement of its efficiency and thus numerical simulation is a key technique that will enable us to understand the operational mechanisms of PSCs [10]. The simulation will further help prognosticate the maximum value of the solar cell with controlled design. Therefore, the aim of this study was to employ SCAPS-1D software [11] to obtain optimum thicknesses for the window layer and absorber in order to enhance $CH_3NH_3PbI_{3-x}Cl_x$ power conversion efficiency. The interface of layers is known to affect the photovoltaic performance of

the solar cells, but in the present study, its effect was not considered.

1.1. Numerical Model for the Perovskite Solar Cell and Material Parameters. The designing and characterizing of the $CH_3NH_3PbI_{3-x}Cl_x$ PSC model was done using the simulation tool SCAPS-1D version 3.3.07 ("SCAPS3307") [11]. The SCAPS software has the ability to solve the fundamental semiconductor equations; the Poisson equations, the continuity equations for electrons and holes, and carrier transport [12]. The working point conditions of the SCAPS simulations were temperature 300 K, work point bias voltage 0 V, and frequency of 1.0×10^6 Hz. The influence of variation of temperature and the surrounding such as moisture of inert gas was not studied. However, as reported by Usha et al. [13], an increase in temperature beyond 300 K would lead to a drastic decrease in the solar cell performance. The simulation was done under AM1_5G 1 sun spec.

The cell structure consists of FTO/TiO_2 multilayer films on glass substrate, $CH_3NH_3PbI_{3-x}Cl_x$ absorber layer, a Spiro-OMeTAD hole transport layer, and silver back contact as shown in Figure 1. Fluorine doped tin oxide (FTO) acts as transparent conducting oxide (TCO) as well as the front electrode and titanium dioxide (TiO_2) as electron transport material (ETM). FTO was chosen over ITO since it demonstrates special features in chemical inertness, stability to heat treatment, mechanical hardness, its large conductivity, it is less expensive, as well as the sheet resistance of ITO increases during sintering whereas that of FTO remains constant [14–17]. Further, tin oxide films are highly transparent in the visible range [18].

The layer parameters employed in the simulation were extracted from the literature [19–21] and summarized in Table 1. Figure 2 shows the energy band structure for the solar cell obtained from SCAP-1D software. It is observed from the structure that the cell can absorb most of the radiations from the sun for the absorber with a lower bandgap. Therefore, more holes and electrons will be generated and consequently more current generated. The improved current flow will lead to an increasement of fill factor and efficiency [10]. The device output performance was majorly based on the electrical, optical, material, and device parameters that were used in the simulation. In an endeavor to attain more practical results, the bulk defects in each layer were introduced as illustrated in Table 2.

2. Results and Discussion

2.1. Effect of FTO Thickness. A transparent conducting oxide (TCO) plays an important role in a solar cell since it is employed as the front electrode as well as a backside reflector [22]. Therefore, the influence on the variation of FTO thickness on the performance of $CH_3NH_3PbI_{3-x}Cl_x$ PSC was studied. Figures 3 show the analysis of the performance cell, i.e., V_{oc}, J_{sc}, FF, and PCE of $CH_3NH_3PbI_{3-x}Cl_x$ PSC as functions of FTO thickness varied from 100 nm to 450 nm, while keeping other layer parameters constant.

Figure 3(a) shows that open-circuit voltage does not change with an increase in FTO thickness, whereas short-circuit current density decreases from 26.18% to 26.07% when FTO thickness is increased from 100 nm to 450 nm. The increase in FTO thickness leads to increased optical absorption of incident light in the layer at the front side of the cell which in turn leads to internal scattering, prolonging the path of light [23, 24]. Therefore, the increased absorption leads to a decrease in the amount of the photons reaching the absorber layer which reduces the amount of current generated, and consequently the short-circuit current decreases. The constant V_{oc} observed is because the major process in photovoltaic is excitation of charges, which occurs in the absorber layer. The Fermi level splitting within the $CH_3NH_3PbI_{3-x}Cl_x$ absorber layer is within the band edges of FTO, thus V_{oc} of the cell remains constant.

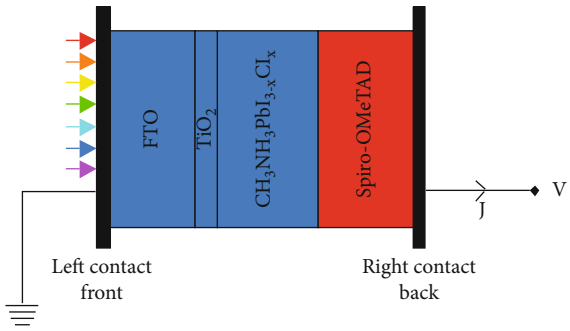

Figure 1: $CH_3NH_3PbI_{3-x}Cl_x$ perovskite solar cell architecture.

Figure 3(b) shows a negligible improvement of FF from 70.77% to 70.80% as the FTO thickness increase from 100 nm to 450 nm. On the other hand, PCE decreases with an increase in FTO thickness. The decrease in efficiency is associated with a decrease in J_{sc} as explained above. This decrease in J_{sc} can also be explained in terms of charge extraction. The generated charges need to have a longer lifetime to be extracted through the FTO but that is not possible. Consequently, there is an increase in charge recombination occurring at the FTO and at the FTO/TiO2 interface as a result of an increase in diffusion length with an increase in FTO thickness. Therefore, from the above simulation, it is clear that a 100 nm thick FTO will significantly improve the performance of $CH_3NH_3PbI_{3-x}Cl_x$ PSC.

2.2. Effect of TiO_2 Thickness. TiO_2 plays a key role in the performance of the device in transporting the generated electrons while blocking the holes from reaching the FTO electrode. Its thickness was varied from 5 nm to 50 nm while maintaining other layer parameters constant. The results obtained are as shown in Figures 4. Figure 4(a) shows open-circuit voltage and short-circuit current density as functions of TiO_2 thickness while Figure 4(b) shows the fill factor and solar cell efficiency as functions of TiO_2 thickness.

It is observed from Figures 4 that there is no significant change in J_{sc}, V_{oc}, FF, and η as TiO_2 thickness increases from 5 nm to 50 nm. Although, there were no significant changes observed, a 5-50 nm thick TiO_2 gave an average of 26.18 mA/cm^2, 1.25 V, 70.77%, and 23.10% for J_{sc}, V_{oc}, FF, and η, respectively. The observation implies that the buffer thickness between 5 nm and 50 nm have no much effect on

Table 1: Layer parameters used for simulation Perovskite solar cells.

Solar cell parameter	FTO	TiO_2	$CH_3NH_3PbI_{3-x}Cl_x$	Spiro-OMeTAD
Band gap, E_g (eV)	3.6	3.26	1.55	3.0
Thickness, t (μm)	0.2 (varied)	0.05	0.6 (varied)	0.35
Electron affinity, χ_e (eV)	4	4.26	3.9	2.45
Relative dielectric permittivity, ε_r.	9	10	30	3
NC effective density (cm-3)	2.2×10^{18}	2.2×10^{18}	2.2×10^{18}	2.2×10^{18}
N_D effective density (cm^{-3})	1.8×10^{19}	1.8×10^{19}	1.8×10^{19}	1.8×10^{19}
Electron thermal velocity (cm/s)	1.0×10^{7}	1.0×10^{7}	1.0×10^{7}	1.0×10^{7}
Hole thermal velocity (cm/s)	1.0×10^{7}	1.0×10^{7}	1.0×10^{7}	1.0×10^{7}
Electron mobility, μ_n (cm^2/Vs)	20	20	2	2.0×10^{-4}
Hole mobility, μ_p (cm^2/Vs)	10	10	2	2.0×10^{-4}
Carrier density of the donor, N_D (cm^{-3})	1.0×10^{18}	5.0×10^{17}	1.0×10^{13}	—
Carrier density of the acceptor, N_A (cm^{-3})	—	—	1.0×10^{12}	2.0×10^{18}

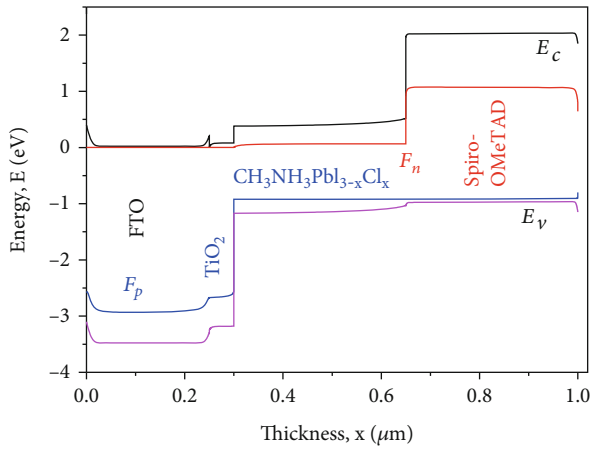

Figure 2: Energy band structure for the solar cell.

the device performance. TiO_2 thickness of more than 50 nm may have deteriorating solar cell properties as reported by Odari et al. [20]. Due to fabrication challenges, we chose 50 nm thick TiO_2 as our optimum value which agrees with experimental work [25].

2.3. Effect of $\mathbf{CH_3NH_3PbI_{3-x}Cl_x}$ *Thickness.* The efficiency of the device majorly depends on the absorber thickness, and therefore the cell was simulated to determine the influence of variation in $CH_3NH_3PbI_{3-x}Cl_x$ thickness on open-circuit voltage (V_{oc}), short-circuit current density (J_{sc}), fill factor (FF), and power conversion efficiency (PCE). $CH_3NH_3PbI_{3-x}Cl_x$ thickness was varied from 100 nm to 1200 nm while keeping other layer parameters constant. The results obtained are as shown in Figures 5. Figure 5(a) shows open-circuit voltage and current density as functions of $CH_3NH_3PbI_{3-x}Cl_x$ thickness, while Figure 5(b) shows the fill factor and efficiency of the solar cell as functions of $CH_3NH_3PbI_{3-x}Cl_x$ thickness.

It is observed from Figure 5(a) that short circuit-current density increases with the increase of $CH_3NH_3PbI_{3-x}Cl_x$ thickness from 100 nm to 300 nm and slightly levels from 300 nm to 1200 nm. The J_{sc} increases rapidly from 24.69% to 26.02% for a thickness from 100 nm to 300 nm. The J_{sc} majorly relies on the production of the charge carriers. The increase of $CH_3NH_3PbI_{3-x}Cl_x$ thickness leads to an increase in the absorbed light and carrier concentration which consequently leads to increment in short-circuit current. The increase in J_{sc} can also be associated with a high absorption coefficient (10^{15} cm^{-1}) of the $CH_3NH_3PbI_{3-x}Cl_x$ layer [26]. The flattening of J_{sc} curve after 300 nm implies that at this point all light is absorbed [27]. On the other hand, there is a significant decrease of open-circuit voltage with an increase of $CH_3NH_3PbI_{3-x}Cl_x$ thickness from 100 nm to 1200 nm. The decrease of V_{oc} implies that the absorber thickness increases the recombination current since in thicker absorber devices, carrier charges generated near the centre of $CH_3NH_3PbI_{3-x}Cl_x$ layer recombines when the thickness surpasses the diffusion length. Further, the increase of $CH_3NH_3PbI_{3-x}Cl_x$ thickness leads to the reduction of its effective bandgap which consequently leads to a reduction in V_{oc} [27, 28].

From Figure 5(b), it is observed that the fill factor decreases incessantly from 75.88% to 68.53% as $CH_3NH_3PbI_{3-x}Cl_x$ thickness increases from 100 nm to 1200 nm. The fill factor mainly is associated with resistive losses and the shape of the J-V curve [26]. Resistance increases with the increase in absorber thickness which consequently leads to a decrease in FF [27]. The same trend is observed with the efficiency curve since the increase in absorber thickness leads to an increment of recombination and reduction in the extraction rate of charge carriers [13]. Since, J_{sc} curve starts to flatten at around 300 nm, our simulation shows that an absorber thickness from 300 nm to 400 nm is suitable. Therefore, a 300 nm-thick $CH_3NH_3PbI_{3-x}Cl_x$ showed an improved device performance.

The major task of the simulation was to optimize the FTO, TiO_2, and $CH_3NH_3PbI_{3-x}Cl_x$ thicknesses which would give an improved performance of $CH_3NH_3PbI_{3-x}Cl_x$ PSC with the structure glass/FTO/TiO_2/$CH_3NH_3PbI_{3-x}Cl_x$/Spiro-OMeTAD/Ag. From the analysis above, it was

Table 2: The defect parameters for the Gaussian distribution.

	FTO	TiO_2	$CH_3NH_3PbI_{3-x}Cl_x$	Spiro-OMeTAD
Type	Neutral	Neutral	Neutral	Neutral
Density defects (cm^{-3})	$1 \times 10^{+15}$	$1 \times 10^{+15}$	$2.5 \times 10^{+13}$	$1 \times 10^{+15}$
Electron capture cross-section (σ_n)	1×10^{-15}	1×10^{-15}	1×10^{-15}	1×10^{-15}
Hole capture cross-section (σ_p)	1×10^{-15}	1×10^{-15}	1×10^{-15}	1×10^{-15}
Energy (eV)	Above E_V	Above E_V	Above E_V	Above E_V

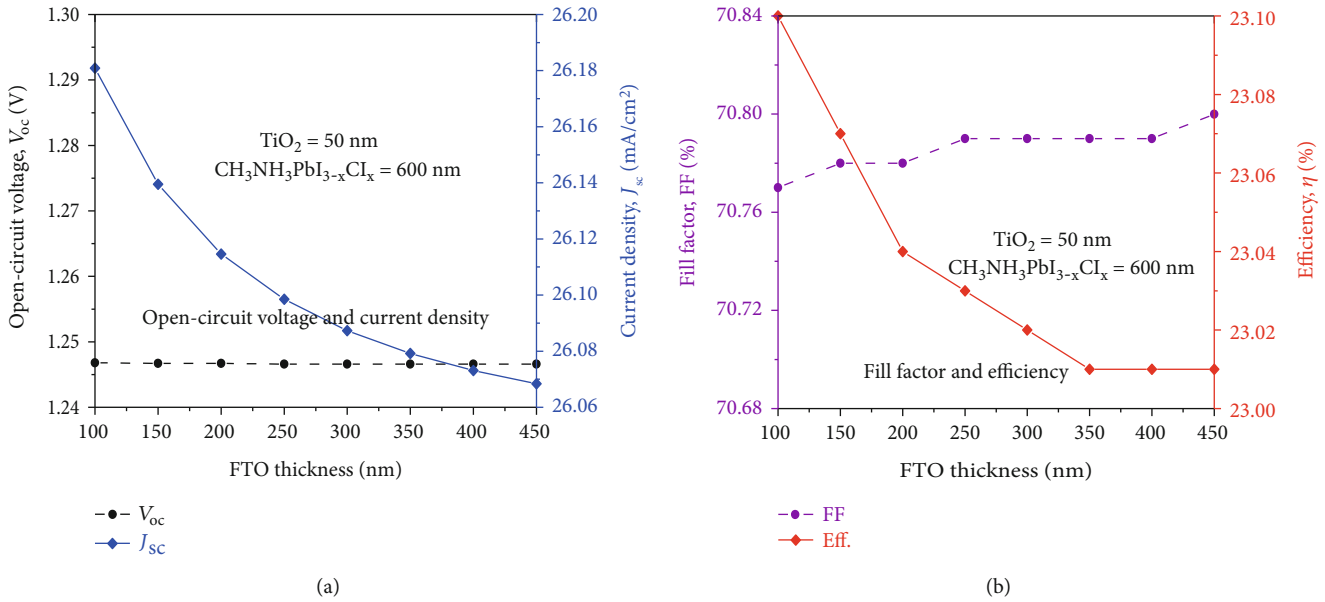

Figure 3: (a) Open-circuit and current density (b) fill factor and efficiency as functions of FTO thickness for constant TiO_2 and $CH_3NH_3PbI_{3-x}Cl_x$ thicknesses.

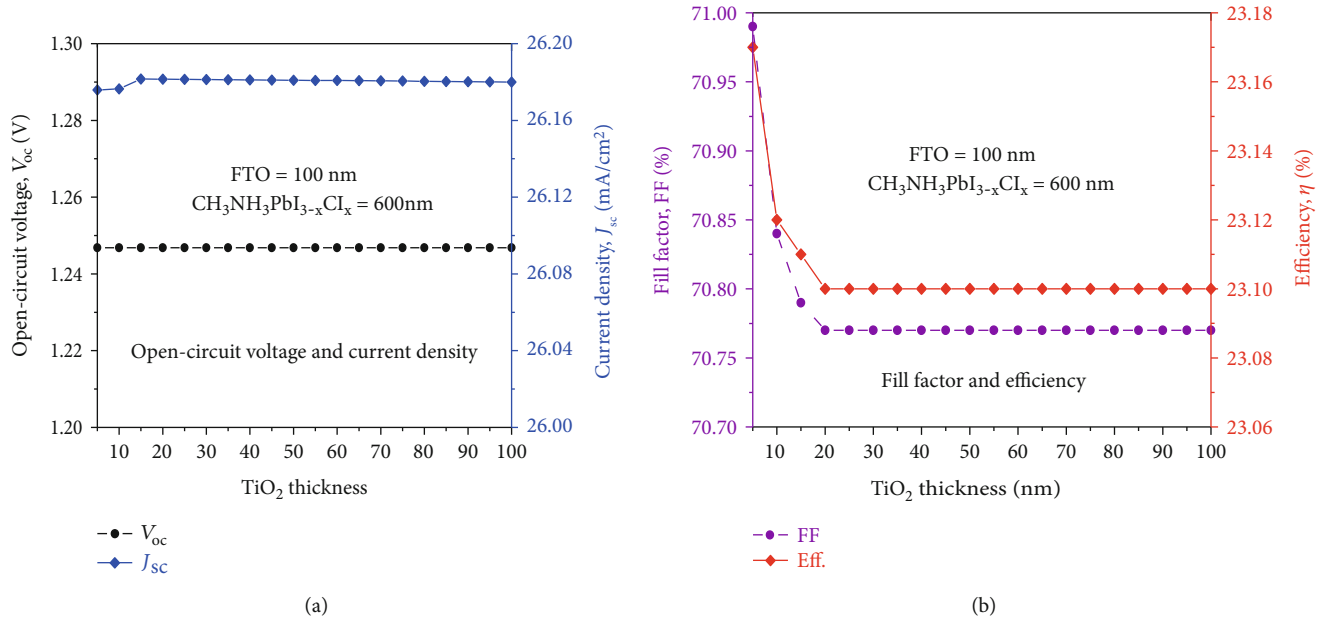

Figure 4: (a) Open-circuit and current density (b) fill factor and efficiency as functions of TiO_2 thickness for constant FTO and $CH_3NH_3PbI_{3-x}Cl_x$ thicknesses.

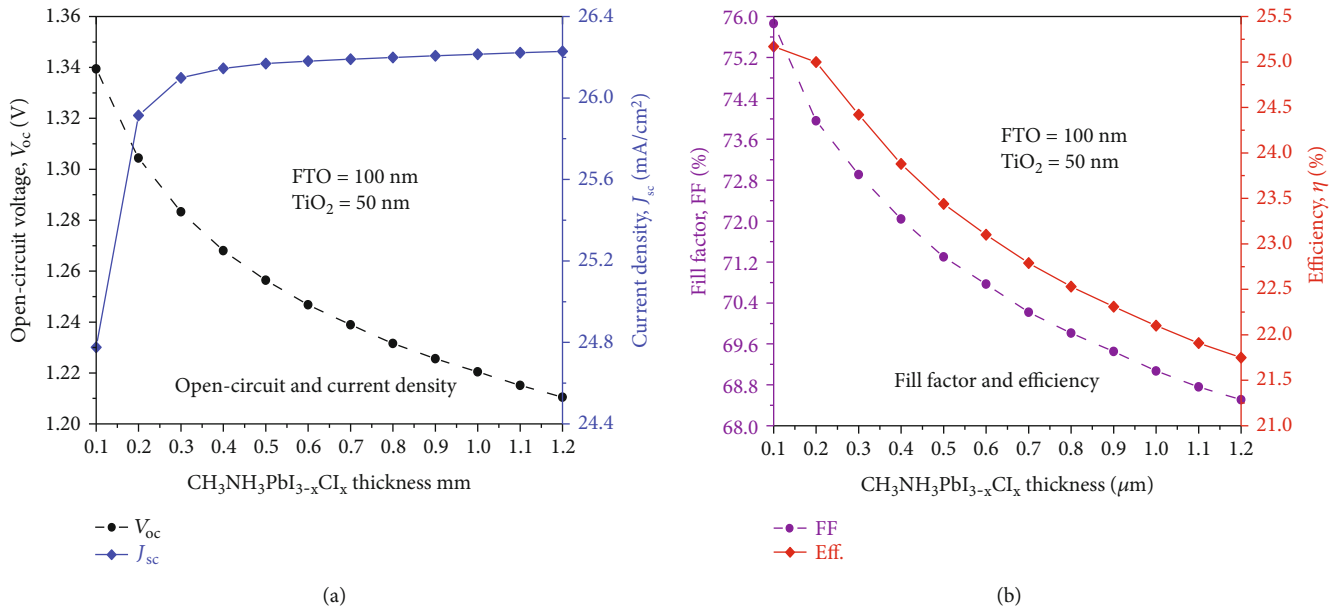

Figure 5: (a) Open-circuit and current density (b) fill factor and efficiency as functions of $CH_3NH_3PbI_{3-x}Cl_x$ thickness for constant FTO and TiO_2 thicknesses.

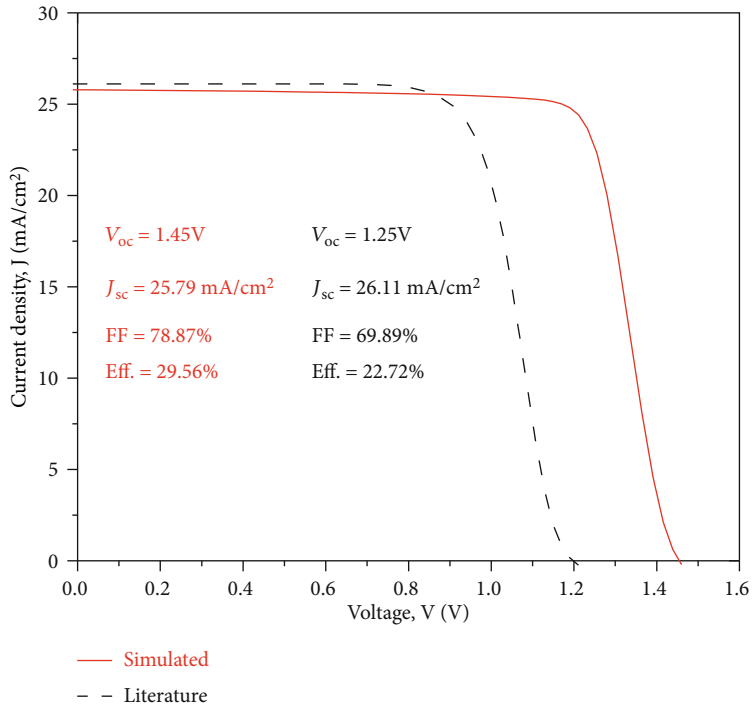

Figure 6: J-V characteristics of the cell.

observed that 100 nm, 50 nm, and 350 nm layer thicknesses for FTO, TiO_2, and $CH_3NH_3PbI_{3-x}Cl_x$, respectively, gave a better cell performance. Therefore, with these layer thicknesses, the J-V characteristics curve of the solar cell was computed and the result is as shown in Figure 6. From the J-V computation, a higher efficiency of 29.56% was attained which is an improvement from the one already reported value [10]. Also, a high open-circuit voltage of 1.45 V is achieved which is also an improvement of an experimental value (1.25 V) already reported [29]. Furthermore, the FF of 78.87% was attained. The high value implies better absorption of solar radiations in the absorber material.

3. Conclusion

In this work, the perovskite solar cell with the structure glass/FTO/TiO_2/$CH_3NH_3PbI_{3-x}Cl_x$/Spiro-OMeTAD/Ag was successively simulated using SCAPS-1D software. FTO, TiO_2, and $CH_3NH_3PbI_{3-x}Cl_x$ thicknesses were varied to investigate their influence on the device performance. The simulation revealed that the variation of TiO_2 thickness has no significance change in the device performance, and an absorber thickness from 300 nm to 400 nm is suitable for better device performance and hence thicker absorber may have no much advantages. The simulation results further revealed that 100 nm, 50 nm, and 300 nm layer thicknesses for FTO, TiO_2, and $CH_3NH_3PbI_{3-x}Cl_x$, respectively, gave a better cell performance as compared to 200 nm, 50 nm, and 600 nm layer thicknesses for FTO, TiO_2, and $CH_3NH_3PbI_{3-x}Cl_x$ reported in the literature.

Data Availability

The [layer parameters used in simulation] data used to support the findings of this study are included in the article.

Conflicts of Interest

The authors declare that there is no conflict of interest regarding the publication of this article.

Acknowledgments

The authors most sincerely appreciate Dr. Marc Burgelman and his staff at the University of Gent, Belgium, for the freely distributed SCAPS-1D simulator. The authors also thank the Computational and Theoretical Physics (CTheP), Masinde Muliro University of Science and Technology group for the computation facilities.

References

[1] S. Shafiee and E. Topal, "When will fossil fuel reserves be diminished?," *Energy Policy*, vol. 37, no. 1, pp. 181–189, 2009.

[2] F. Barbir, T. Veziroglu, and H. Plassjr, "Environmental damage due to fossil fuels use," *International Journal of Hydrogen Energy*, vol. 15, no. 10, pp. 739–749, 1990.

[3] P. Zhao et al., "Device simulation of inverted CH3NH3PbI3 −xClx perovskite solar cells based on PCBM electron transport layer and NiO hole transport layer," *Solar Energy*, pp. 11–18, 2018.

[4] A. A. Said, J. Xie, Y. Wang et al., "Efficient Inverted Perovskite Solar Cells by Employing N-Type (D–A 1 –D–A 2) Polymers as Electron Transporting Layer," *Small*, vol. 15, no. 29, p. 1803339, 2019.

[5] H.-S. Kim, S. H. Im, and N.-G. Park, "Organolead halide perovskite: new horizons in solar cell research," *The Journal of Physical Chemistry*, vol. 118, no. 11, pp. 5615–5625, 2014.

[6] M. Osborne, *Oxford PV Takes Record Perovskite Tandem Solar Cell to 27.3% Conversion Efficiency*, Manufacturing, Materials, Cell Processing, Thin-Film, Europe, 2018.

[7] A. A. Said, J. Xie, and Q. Zhang, "Recent Progress in Organic Electron Transport Materials in Inverted Perovskite Solar Cells," *Small*, vol. 15, no. 27, p. 1900854, 2019.

[8] P.-Y. Gu, N. Wang, A. Wu et al., "An azaacene derivative as promising electron-transport layer for inverted perovskite solar cells," *Chemistry - An Asian Journal*, vol. 11, no. 15, pp. 2135–2138, 2016.

[9] R. Wei, *Modelling of Perovskite Solar Cells*, Queensland University of Technology, Brisbane, 2018.

[10] H. Faruk, M. Faisal, and H. Okada, *"Device Modelling and Performance Analysis of Perovskite Solar Cells Based on Similarity with Inorganic Thin Film Solar Cells Structure," in Electrical*, Computer & telecommmunication Engineering, Bangledesh, 2016.

[11] M. Burgelman, P. Nollet, and S. Degrave, "Modelling polycrystalline semiconductor solar cells," *Thin Solid Films*, vol. 361-362, pp. 527–532, 2000.

[12] H. Movla, "Optimization of the CIGS based thin film solar cells: numerical simulation and analysis," *Optik*, vol. 125, no. 1, pp. 67–70, 2014.

[13] M. Usha, S. Vedanayakam, and K. Thyagarajan, "Numerical simulation of Ch3Nh3PbI3-XClx perovskite solar cell using SCAPS-1D," *International Journal of Engineering Science Invention*, pp. 40–45, 2017.

[14] R. Mishra, K. Sheo, and S. Prakash, "Optical and gas sensing characteristics of tin oxide nano-crystalline film," *Journal of Ovonic Research*, pp. 77–85, 2009.

[15] K. S. Shamala, L. C. S. Murthy, and K. Narasimha Rao, "Studies on tin oxide films prepared by electron beam evaporation and spray pyrolysis methods," *Bulletin of Materials Science*, vol. 27, no. 3, pp. 295–301, 2004.

[16] M. Umer, R. Saleem-ur, H. Khalil, A. Ibnelwaleed, and B. Reddy, "Recent advances in dye sensitized solar cells," *Advances in Materials Science and Engineering*, 12 pages, 2014.

[17] A. Andersson, N. Johansson, P. Bröms, N. Yu, D. Lupo, and W. R. Salaneck, "Fluorine tin oxide as an alternative to indium tin oxide in polymer LEDs," *Advanced Materials*, vol. 10, no. 11, pp. 859–863, 1998.

[18] C. Agashe, M. G. Takwale, V. G. Bhide, S. Mahamuni, and S. K. Kulkarni, "Effect of Sn incorporation on the growth mechanism of sprayed SnO2films," *Journal of Applied Physics*, vol. 70, no. 12, pp. 7382–7386, 1991.

[19] F. Hossain, M. Faisal, and H. Okada, "Device modeling and performance analysis of perovskite solar cells based on similarity with inorganic thin film solar cells structure," in *2016 2nd International Conference on Electrical, Computer & Telecommunication Engineering (ICECTE),*, Bangladesh, 2016.

[20] V. Odari, R. Musembi, and J. Mwambora, "Device simulation of Sb2S3 solar cells by SCAPS-1D software," *African Journal of Physical Sciences*, vol. 3, pp. 39–54, 2019.

[21] A. Husainat, W. Ali, P. Cofie, J. Attia, and J. Fuller, "Simulation and analysis of methylammonium lead iodide ($CH_3NH_3PbI_3$) perovskite solar cell with Au contact using SCAPS 1D simulator," *American Journal of Optics and Photonics*, vol. 7, no. 2, p. 33, 2019.

[22] M. Joachim, R. Bernd, J. Springer, and M. Vanecek, "TCO and light trapping silicon thin film solar cells," in *Science Direct*, vol. 77, pp. 917–930, Elsevier, 2004.

[23] R. Gordon, "Criteria for choosing transparent conductors," *MRS Bulletin*, vol. 25, no. 8, pp. 52–57, 2000.

[24] M. Chadel, M. M. Bouzaki, A. Chadel, M. Aillerie, and B. Benyoucef, "Thickness optimization of the ZnO based TCO layer in a CZTSSe solar cell. evolution of its performance

with thickness when external temperature changes," *Journal of Physics: Conference Series*, vol. 879, p. 012006, 2017.

[25] T. Nakada and M. Mizutani, "18% Efficiency Cd-Free Cu(In, Ga)Se2 Thin-Film Solar Cells Fabricated Using Chemical Bath Deposition (CBD)-ZnS Buffer Layers," *Japanese Journal of Applied Physics*, vol. 41, pp. L165–L167, 2002.

[26] N. Devi, K. A. Parrey, A. Aziz, and S. Datta, "Numerical simulations of perovskite thin-film solar cells using a CdS hole blocking layer," *Journal of Vacuum Science & Technology B*, vol. 36, no. 4, p. 04G105, 2018.

[27] A. Bag, R. Radhakrishnan, R. Nekovei, and R. Jeyakumar, "Effect of absorber layer, hole transport layer thicknesses, and its doping density on the performance of perovskite solar cells by device simulation," *Solar Energy*, vol. 196, pp. 177–182, 2020.

[28] L. M. Pazos-Outón, T. P. Xiao, and E. Yablonovitch, "Fundamental efficiency limit of lead iodide perovskite solar cells," *Journal of Physical Chemistry*, vol. 9, no. 7, pp. 1703–1711, 2018.

[29] J. Burschka, N. Pellet, S.-J. Moon et al., "Sequential deposition as a route to high-performance perovskite-sensitized solar cells," *Nature*, vol. 499, no. 7458, pp. 316–319, 2013.